

The dependence of frequency upon microwave power of wall-coated and buffer-gas-filled gas cell Rb⁸⁷ frequency standards

A. Risley and S. Jarvis, Jr.
National Bureau of Standards, Boulder, Colorado

J. Vanier
Laboratoire d'Electronique Quantique, Département de Génie Electrique, Université Laval, Québec, Canada

(Received 28 September 1979; accepted for publication 10 June 1980)

Previous studies of a commercial passive gas cell Rb⁸⁷ frequency standard showed a strong dependence of the output frequency ν_{Rb} upon the microwave power $P_{\mu\lambda}$. A major conclusion of that work was that the dependence of ν_{Rb} upon $P_{\mu\lambda}$ was due to a line inhomogeneity effect. The line inhomogeneity interpretation suggested that substituting a wall coating for the usual buffer gas would reduce the dependence upon $P_{\mu\lambda}$. As a part of the present work, a wall coating (a form of paraffin) was used and a reduction of this dependence by a factor of 100 was obtained. The present work has led to a more convincing theoretical demonstration of the line inhomogeneity effect. The paper discusses some of the details of the analytical procedure. There are certain major requirements that a wall coating would have to satisfy if it is to be superior to the usual buffer gas, and these are discussed in the text. The advantages demonstrated by the present work indicate that further studies are warranted to determine if an improved standard could be built based on a wall coating.

PACS numbers: 06.30.Ft

BACKGROUND

The passive Rb⁸⁷ gas cell frequency standard is the most prevalent type of atomic frequency standard in the field. Its good frequency stability has made it suitable for a great number of applications. The results of the work reported here suggest that the use of a wall coating instead of the usual buffer gas might improve its medium and long term frequency stability.

Earlier work on a prevalent commercial Rb⁸⁷ standard demonstrated a very strong frequency dependence upon the microwave power $P_{\mu\lambda}$.¹ This effect appears to be due to a combination of relatively immobile Rb⁸⁷ atoms and a frequency gradient across the absorption cell. The immobility is due to the use of a buffer gas in the cell.

The work reported here demonstrates that substituting a wall coating for the buffer gas results in a drastically reduced dependence of the output frequency ν_{Rb} upon $P_{\mu\lambda}$. In the commercial unit studied in Ref. 1, the dependence upon $P_{\mu\lambda}$ caused by the line inhomogeneity was *probably* the predominant cause of frequency instability for averaging times of the order of one month and longer. Thus the ability to use wall coating in lieu of buffer gas might be important commercially.

In the following text we discuss the experimental results of the present work. Next we give results of the line inhomogeneity analysis which represents our understanding of the dependence of ν_{Rb} upon $P_{\mu\lambda}$ when a buffer gas is used. Finally, we discuss some advantages and disadvantages of using wall coatings.

EXPERIMENTAL RESULTS

Experimental setup

The experimental arrangement used in these experiments is shown in Fig. 1. An optical package capable of giving

ing a strong resonance of the $F = 2, M_F = 0$ to $F = 1, M_F = 0$ transition was used to lock the frequency of a crystal oscillator driving a frequency synthesizer. The frequency was measured with a counter. The arrangement gave a resolution of 1×10^{-10} which was sufficient for the types of phenomena studied. The optical package, consisting of a rubidium 87 lamp, an isotopic filter, and a TE₀₁₁ exciting cavity, was equipped with a special cell. This cell, made of quartz, was coated with a form of paraffin and connected to a vacuum system. It contained a few milligrams of rubidium 87 in a tail, whose temperature could be controlled independently of the cavity. In our work the temperature was 70 °C. The cell was 3.2 cm in diameter and was held at 71 °C. The cavity was 5.7 cm in diameter and about 7 cm long. The Q of this cavity was sufficiently high that a cavity pulling effect could

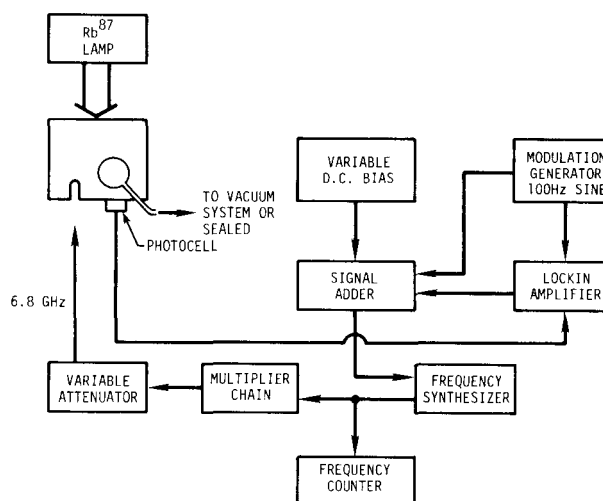


FIG. 1. A schematic of the measurement system.

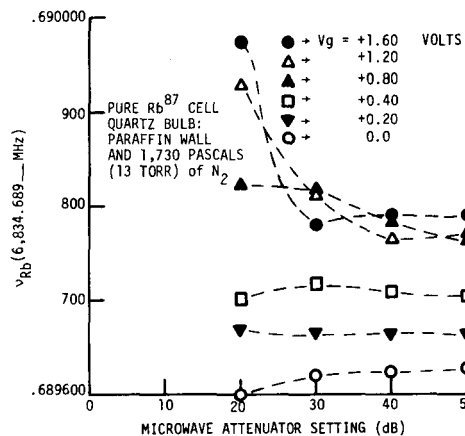


FIG. 2. The output frequency ν_{Rb} vs applied microwave power for a cell filled with 1730 Pa (13 Torr) of N_2 . Minimum microwave power corresponds to an attenuator setting of 50 dB. The voltage applied to the gradient coils is the parameter. A voltage V_g of 1.6 V applied to the gradient coils causes a frequency change of about 2500 Hz across the cell.

be observed, although the system was operated in the passive mode. These results will be reported elsewhere.²

In order to study the effects of power shift in the presence of frequency gradients across the cell, special coils were mounted at the end of the cavity. These coils were about 4.5 cm in diameter and were separated by 7 cm. Each consisted of 150 turns. The coils produced a magnetic field gradient which was then translated by the rubidium 87 atomic ensemble to a frequency gradient. The effect of gradients of this sort could then be studied under controlled conditions, and in circumstances where the atom was free to average the magnetic gradient and light shift, in the case of the coated cells, or where the atoms were fixed in space with a buffer gas. In this last case, the field gradient and light shift are not averaged by the atomic motion and spatially inhomogeneous broadening and shifting of the resonance line occurs. This shifting and broadening depends on the level of $P_{\mu\lambda}$, and thus the frequency dependence upon $P_{\mu\lambda}$ results.

RESULTS

ν_{Rb} versus $P_{\mu\lambda}$ and magnetic gradient

Figure 2 shows ν_{Rb} versus $P_{\mu\lambda}$, using 1730 Pa (13 Torr) of N_2 as buffer gas, with the voltage applied to the gradient coils as a parameter. The level of $P_{\mu\lambda}$ is determined by the microwave attenuator and, for an attenuator setting of 50 dB, the power absorbed by the cavity is approximately 1×10^{-10} W. The data of Figs. 2 through 5 were taken with the cavity frequency tuned to within ± 25 kHz of ν_{Rb} . Based on our cavity pulling measurements, we conclude that the worst case pulling of ν_{Rb} would be no more than 0.25 Hz due to this offset. Since the precision of the frequency measurements is about 0.7 Hz, cavity pulling effects are negligible. The dashed lines on these figures are solely for the unambiguous identification of the points.

The resonant frequency of any given atom has a quadratic dependence upon the magnetic field and the coils produce a linear field gradient across the cell. For the maximum

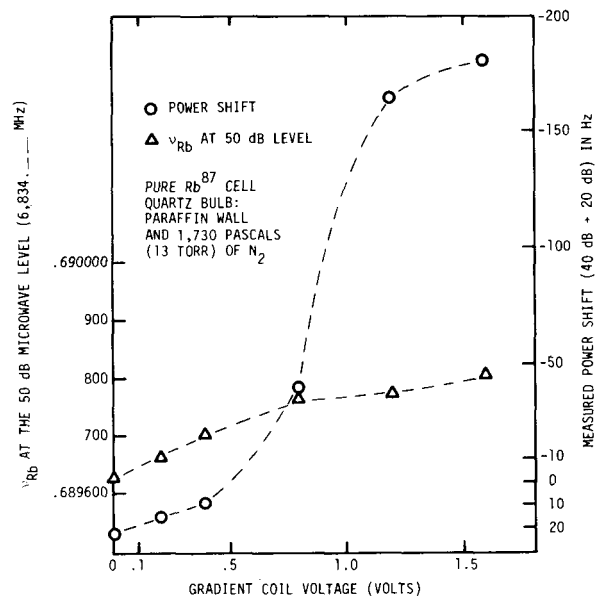


FIG. 3. The data shown in this figure was taken on the same cell as used in Fig. 2. The right-hand ordinate represents a frequency change due to a 20-dB change in microwave power $P_{\mu\lambda}$. The abscissa is the voltage applied to the gradient coils and is a measure of the frequency gradient across the cell. The left-hand ordinate is the output frequency at the $P_{\mu\lambda} = 50$ -dB level.

voltage (1.6 V) applied to the gradient coils, the resonant frequencies of the atoms vary across the cell by about 2500 Hz. This is, of course, a much larger gradient than would be encountered in a working standard. The purpose of applying such a large gradient was twofold. First, since the spatial variation of the magnetic gradient is more accurately known than that of the light shift, we wanted to have a condition where the total gradient was primarily due to the magnetic gradient. Second, we wanted to clearly show the dramatic

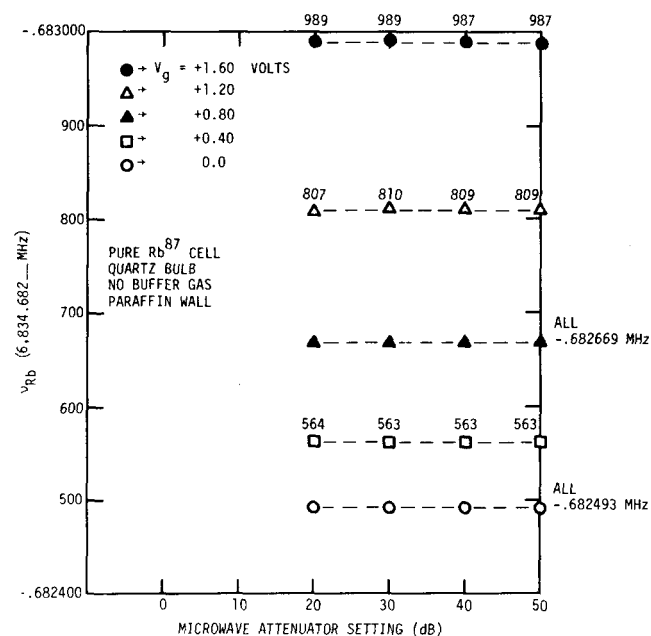


FIG. 4. Same as for Fig. 2 except that the cell wall was coated with paraffin and the cell was kept under vacuum.

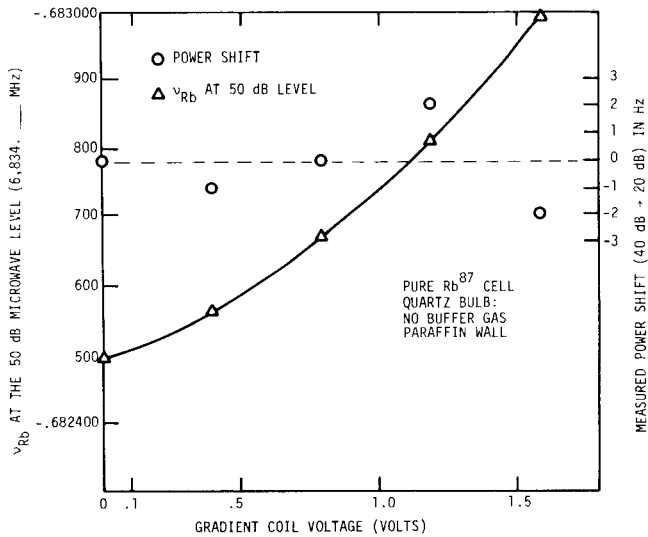


FIG. 5. Same cell as for Fig. 4. The two ordinates and the abscissa are the same as for Fig. 3.

change in sensitivity to $P_{\mu\lambda}$ when the buffer gas is removed. On the other hand, for applied gradient voltages less than about 0.2 V, the light shift gradient dominates.

In Fig. 3 we have plotted the data in a different form. On the right ordinate scale, to emphasize the change in frequency with change in power, we have plotted a frequency change due to a 20-dB change in $P_{\mu\lambda}$ versus the gradient voltage. The microwave change is from an attenuator setting of 40 dB to one of 20 dB.³ This change in $P_{\mu\lambda}$ is, of course, vastly larger than would be encountered in normal operating conditions, and our purpose was to emphasize the difference between a buffer-gas-filled cell and one with only a wall coating. Also shown in Fig. 3 on the left ordinate is the resonant frequency as a function of applied gradient voltage at a 50-dB attenuation setting for the microwave power. Figures 4 and 5 give the same information for the paraffin coated, unsealed cell attached to the vacuum system.

The data reported in Fig. 4 for the cell without a buffer gas can be directly compared to the data shown in Fig. 2 for the cell containing a buffer gas. In the first case, it is observed that there is a practically no dependence of the frequency upon microwave power. This is made more evident in Fig. 5 through the curve identified as "power shift." It is concluded from this data the rapid motion of the rubidium atoms produces an averaging of the inhomogeneities across the cell, in the case of the storage cell not containing a buffer gas; this motion reduces drastically the inhomogeneous broadening.

TABLE I. Limiting linewidth versus cell type.

Type of cell (2.5 cm diam.)	$\Delta\nu_{Rb}$ (Hz)
Paraffin coated cell with 1730 Pa of N_2	170
Paraffin coated cell without buffer gas	230

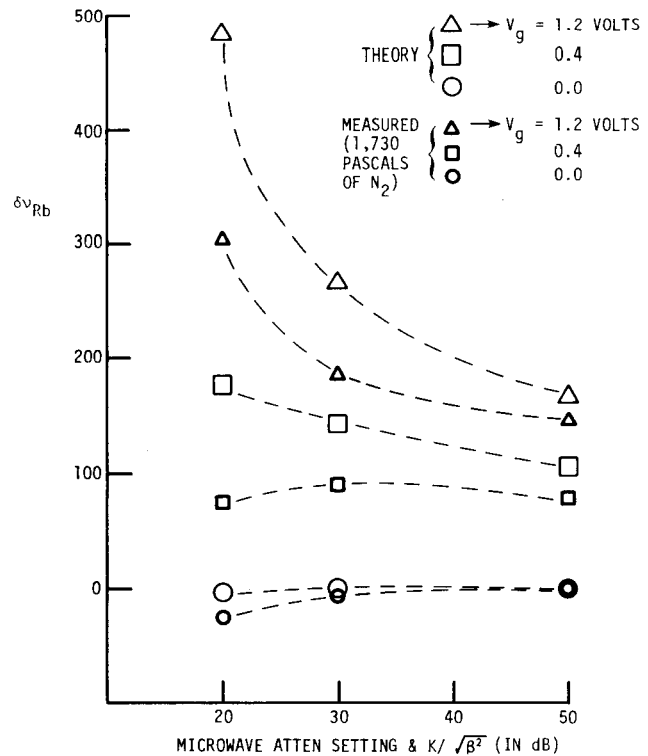


FIG. 6. The theoretically obtained frequency change $\delta\nu_{Rb}$ vs $P_{\mu\lambda}$. Also shown for comparison is some of the data of Fig. 2 (expressed as a frequency change).

In the case of the buffer-gas-filled cell, the power shift is very large, as is shown in Fig. 3. This is due to the fact that the rubidium atoms are fixed in space by the buffer gas at least during their time of interaction with the microwave interrogating field; this results in the creation of a strong spatially inhomogeneous broadening. It is further observed that for a certain value of the magnetic field gradient, the power shift goes to zero. This may be interpreted in terms of the opposing effect of the spatially inhomogeneous light shift and of the magnetic field gradient, the light shift producing a positive power shift while the field gradient produces a negative power shift.

The behavior of the absolute frequency as a function of the magnetic field gradient is also observed to be different for the two cases. Although we will not go into details, our analysis shows that this behavior can be explained through considerations of the actual geometry of our system and the spatial distribution of resonance frequencies inside the storage bulb. Experiments done under saturation (20 dB attenuation) have confirmed our assumptions. Calculations give results which are within a factor of 2 of the experimental data.

Linewidth versus $P_{\mu\lambda}$ and pumping light intensity

At the $P_{\mu\lambda} = 20$ -dB level, which is 15–20 dB higher than that which produces the maximum signal, microwave power broadening is responsible for about 60% of the linewidth. In the particular physical arrangement used, the limiting linewidth $\Delta\nu_{Rb}$ was found to be as shown in Table I. These measurements were made under the condition of no

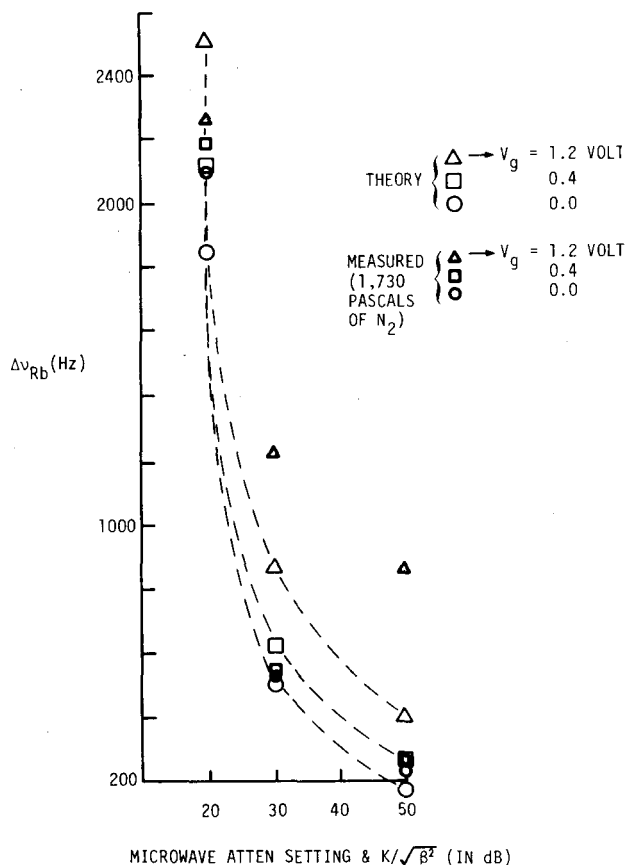


FIG. 7. The theoretically obtained linewidth $\Delta\nu_{Rb}$ vs $P_{\mu\lambda}$. The data shown corresponds to the same cell as in Figs. 2 and 3.

magnetic field gradient, weak light intensity, weak microwave power, and small modulation amplitude.

Further evidence for the validity of the idea of spatial averaging comes from the behavior of $\Delta\nu_{Rb}$ versus magnetic gradient. For example, in standard operating conditions, in the case of the wall-coated cell without buffer gas, $\Delta\nu_{Rb} = 280$ Hz with a gradient voltage of 1.2 V and 260 Hz with no magnetic gradient. For the buffer gas case, at the same level of $P_{\mu\lambda}$ of 50 dB, the values are 850 and 230 Hz. Still further evidence comes from the asymmetry of the line. For the buffer gas case, at 1.2 V gradient voltage, the low-frequency side of the line is 220 Hz wide and the high-frequency side is 630 Hz. On the other hand, without buffer gas, the two sides differ by only 3 Hz, which is less than the precision of the linewidth measurement.

THEORETICAL RESULTS

The theoretical model (for the buffer gas case) assumes that the Rb^{87} atoms are fixed in space and that their resonant frequency depends upon their position within the cell. In the experiment, the buffer gas produces the immobility, with the intentionally applied magnetic gradient plus the spatially changing light shift producing the frequency gradient. Figures 6 and 7 show a comparison between the theory and the data. In these figures, V_g is the voltage applied to the gradient coils; β is the microwave field intensity; K is a constant;

$\delta\nu_{Rb}$ is the change in frequency between the measured (or calculated) value of ν_{Rb} and its value at $V_g = 0$ when the minimum value of microwave field is applied.

The equations used in the present calculations are based upon earlier work done by one of us (JV) and others.⁴⁻⁶ The values of some of the parameters that appear in the equations were determined from our or others measurements. However, the value of pumping light intensity I_0 used in computing Figs. 6 and 7 was obtained by fitting to the data. Approximate values of I_0 , with which to begin, were obtained from Ref. 5.

In our calculation, we have assumed that the intensity I_0 at the input of the cell and absorption line had a Gaussian distribution. Because the pumping light is strongly absorbed as it traverses the cell, as shown in Fig. 8, the light shift varies rapidly along the length of the cell. Based on a measured average light shift of 35 Hz, we estimate a light shift of 100 Hz at the entrance to the cell. Then, by adjusting the offset between the centers of the pumping and absorption lines, we attempted to get agreement with the data for no magnetic gradient ($V_g = 0.0$ of Fig. 6). The calculated values, at $P_{\mu\lambda} = 20$ dB, were typically too small by a factor of 2 or greater. With the probable asymmetry of the spectrum of the pumping light, it does not seem surprising to us that the agreement is poor when the gradient is due primarily to the light shift.

To perform the calculation (since the diameter of the cell is small compared to the diameter of the cavity) we assume that there is no variation of I_0 or β (or of the atom's

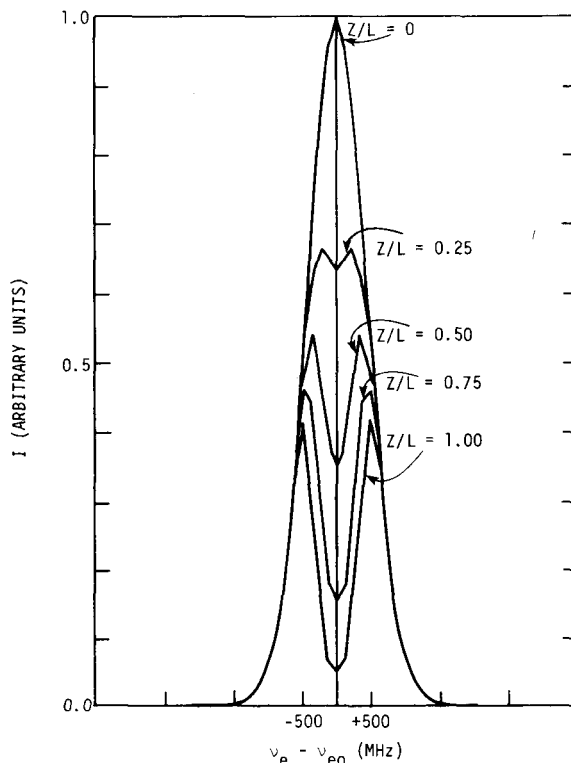


FIG. 8. Calculated (theoretical) pumping light distribution I at several planes along the cell axis. The total length of the cell is L , and Z is measured from the end of the cell where the light enters. The center of the distribution, at $Z = 0$, is at the frequency ν_{e0} .

frequency) across the cell, i.e., at right angles to the axis of the cell. Along the axis we use the distribution for β according to the known mode in the cavity. (In Ref. 1, the Q of the cavity and the cavity configuration were such that β was inadequately known for useful calculations.)

The amplitudes of a discrete (Gaussian-Hermite) spectrum of pumping light frequencies satisfy a system of first-order differential equations in the axial coordinate Z . These were solved numerically by a Runge-Kutta method. The center of the dip in the amplitude distribution is the system frequency ν_{Rb} .

In our technique of measurement, the interrogating microwave signal is frequency modulated and the resonance is detected with a lock-in amplifier. Consequently, a signal closely approximating the derivative of the absorption line is recorded. Thus the measured linewidth $\Delta\nu_{Rb}$ is the width between the inflection points of the absorption line. To make the theoretical procedure compatible with the measurement, the first derivative of the theoretical absorption curve is taken and a theoretical $\Delta\nu_{Rb}$ obtained from the resulting curve.

On the average, the agreement of the theory with the data is sufficiently good to reinforce our belief that the two basic assumptions of the model are correct. On the other hand, there is sufficient uncertainty about the values of the experimental parameters that further attempts to fit the data presented here do not seem warranted.

ADDITIONAL THOUGHTS ON THE USE OF WALL COATINGS

In the work reported in Ref. 1, we found that a change in $P_{\mu\lambda}$ of 0.4 dB about the operation point caused a fractional change in ν_{Rb} of about 1×10^{-11} . The present work shows that, for strong gradients, there is a reduction in the $P_{\mu\lambda}$ dependence by a factor of about 100 due to the use of the wall coating. We presume that (in first order) this factor also holds at weak gradients. Our theoretical model can address

itself to this question, and we are proceeding to do this. A new experimental setup is being prepared which should have measurement precision of a few parts in 10^{13} .

Some of the major questions that need to be answered with regard to wall coatings are: (1) The wall shift in a 2.5-cm-diam bulb is of the order of 200 Hz.^{2,7} Will this frequency shift be sufficiently stable, say one part in 10^{12} or better, over periods of many months? and (2) the temperature coefficient of the present wall coating is of the order of 2 Hz/°C. At present this appears to be large. Will it be possible to find other wall coatings with smaller temperature coefficients?

Despite these uncertainties, the use of a wall coating has made a very large reduction in a major instability. Further studies seem warranted to determine if a significantly improved Rb standard could be developed based on a wall-coated cell.

ACKNOWLEDGMENTS

This work was supported in part by contract SMS-80218, from the Space and Missiles Systems Organization of the U.S. Air Force; the Natural Sciences and Engineering Research Council of Canada; and the Department of Education of the Province of Quebec. The authors would also like to thank Dr. Peter Bender of JILA and Dr. David Wineland of NBS for discussions regarding the data and its implications. One of us (AR) would also like to thank Mr. David Allan of NBS and Dr. Helmut Hellwig, now of Frequency and Time Systems, Inc., for their continued interest and support.

APPENDIX

Equations (1)–(4) represent the theoretical model discussed in the text and are adapted from Refs. 4–6.

$$\frac{d}{dZ} I(Z, \nu) = -\sigma(\nu)n(Z)I(Z, \nu), \quad (A1)$$

$$n(Z) = n_0 \left(\frac{3\gamma_1}{5\Gamma + 8\gamma_1} + \frac{2\beta^2 \Gamma A}{(\frac{5}{8}\Gamma + \gamma_1) \{ [\gamma_1(\omega - \bar{\omega})^2 / (\frac{3}{2}\Gamma + \gamma_2) + \gamma_1(\frac{3}{2}\Gamma + \gamma_2) + 4\beta^2(1 - B) \]} \right), \quad (A2)$$

where

$$A = \frac{\gamma_1(\Gamma + \gamma_1)}{5\Gamma^2 + 13\gamma_1\Gamma + 8\gamma_1^2},$$

$$B = \frac{(3\Gamma + 4\gamma_1)\Gamma}{5\Gamma^2 + 13\gamma_1\Gamma + 8\gamma_1^2}.$$

$I(Z, \nu)$ is the optical flux density given by

$$I(Z, \nu) = Ke^{-\frac{(\nu - \nu_e)^2}{\Delta\nu_e^2}} 4 \ln 2. \quad (A3)$$

Here, K is a constant, ν is the optical pumping frequency, ν_e is the center frequency of the optical emission line, and Z is a measure of distance along the axis of the cavity.

$\sigma(\nu)$ is the cross section for optical absorption. $n(Z)$ is the number of atoms in the lower of the hyperfine states and

is a function of the optical pumping rate Γ , where Γ is defined by

$$\Gamma = \int_{-\infty}^{\infty} d\nu I(Z, \nu) \sigma(\nu).$$

$\beta = \beta_0 \sin(\pi Z / L)$ is the microwave field intensity, β_0 is a constant and L is the length of the cavity. n_0 is the density of Rb⁸⁷ atoms in the cell. γ_1 , a constant, is the rate at which the population difference between the two hyperfine states relaxes. γ_2 , a constant, is the rate at which the microwave-induced coherence between the spins relaxes. ω is the instantaneous angular microwave frequency. $\bar{\omega} = \Omega_0 + \Omega_1 \times H_0^2(Z) + 2\pi l(Z)$ is the angular center frequency of the hyperfine resonance as perturbed by the magnetic field H_0 (Zeeman shift) and the pumping light. The optical pumping

produces an axially dependent frequency shift (the light shift) which is represented by $l(Z)$.

Here, Ω_0 is the unperturbed angular frequency of the hyperfine transition and Ω_1 is a constant.

The optical cross section is given by

$$\sigma(\nu) = \sigma_0 e^{-\frac{(\nu - \nu_a)^2}{\Delta\nu_a^2}} 4 \ln 2, \quad (\text{A4})$$

where σ_0 is a constant and ν_a is the center frequency of the optical absorption.

¹A. Risley and G. Busca, Proc. 32nd Ann. Symp. on Freq. Control, p. 506, 1978 (unpublished).

²A. Brisson, J. Vanier, and A. Risley (unpublished).

³The maximum signal level at the lock-in amplifier occurs for a microwave attenuator setting of about 35 dB. The modulation amplitude (see Fig. 1) used in all these measurements was set to produce a maximum signal level at the lock-in when the frequency of the microwave source was slightly displaced from ν_{rb} . (This is an open loop test.) This is a way of assuring that the microwave source is not being overmodulated.

⁴Jacques Vanier, Phys. Rev. **168**, 129 (1968).

⁵G. Busca, M. Têtu, and J. Vanier, Can. J. Phys. **51**, 1379 (1973).

⁶Gilles Missout and Jacques Vanier, Can. J. Phys. **53**, 1030 (1975).

⁷R. G. Brewer, J. Chem. Phys. **38**, 3015 (1963).